

# ADP ribosylation factor 6 (ARF6) controls amyloid precursor protein (APP) processing by mediating the endosomal sorting of BACE1

Ragna Sannerud<sup>a,b</sup>, Ilse Declerck<sup>a,b</sup>, Aleksandar Peric<sup>a,b</sup>, Tim Raemaekers<sup>a,b</sup>, Guillermo Menendez<sup>c</sup>, Lujia Zhou<sup>b,d</sup>, Baert Veerle<sup>a,b</sup>, Katrijn Coen<sup>a,b</sup>, Sebastian Munck<sup>e</sup>, Bart De Strooper<sup>b,d</sup>, Giampietro Schiavo<sup>c</sup>, and Wim Annaert<sup>a,b,1</sup>

<sup>a</sup>Laboratory of Membrane Trafficking and <sup>d</sup>Laboratory for Research on Neurodegenerative Diseases, Center for Human Genetics, Catholic University of Leuven, and <sup>b</sup>Department of Molecular and Developmental Genetics, Vlaams Instituut voor Biotechnologie, Gasthuisberg, B-3000 Leuven, Belgium; <sup>c</sup>Molecular Neuropathobiology Laboratory, London Research Institute, London, WC2A 3LY, United Kingdom; and <sup>e</sup>Light Microscopy and Imaging Network, Department of Molecular and Developmental Genetics, Vlaams Instituut voor Biotechnologie, Gasthuisberg, B-3000 Leuven, Belgium

Edited by Randy Schekman, University of California, Berkeley, CA, and approved July 8, 2011 (received for review January 14, 2011)

**Amyloid  $\beta$  ( $A\beta$ ) peptides, the primary constituents of senile plaques and a hallmark in Alzheimer's disease pathology, are generated through the sequential cleavage of amyloid precursor protein (APP) by  $\beta$ -site APP cleaving enzyme 1 (BACE1) and  $\gamma$ -secretase. The early endosome is thought to represent a major compartment for APP processing; however, the mechanisms of how BACE1 encounters APP are largely unknown. In contrast to APP internalization, which is clathrin-dependent, we demonstrate that BACE1 is sorted to early endosomes via a route controlled by the small GTPase ADP ribosylation factor 6 (ARF6). Altering ARF6 levels or its activity affects endosomal sorting of BACE1, and consequently results in altered APP processing and  $A\beta$  production. Furthermore, sorting of newly internalized BACE1 from ARF6-positive towards RAB GTPase 5 (RAB5)-positive early endosomes depends on its carboxyterminal short acidic cluster-dileucine motif. This ARF6-mediated sorting of BACE1 is confined to the somatodendritic compartment of polarized neurons in agreement with  $A\beta$  peptides being primarily secreted from here. These results demonstrate a spatial separation between APP and BACE1 during surface-to-endosome transport, suggesting subcellular trafficking as a regulatory mechanism for this proteolytic processing step. It thereby provides a novel avenue to interfere with  $A\beta$  production through a selective modulation of the distinct endosomal transport routes used by BACE1 or APP.**

$\beta$ -site amyloid precursor protein cleaving enzyme 1 (BACE1) is the major  $\beta$ -secretase, and therefore the key rate-limiting factor in the production of amyloid  $\beta$  ( $A\beta$ ) in Alzheimer's disease (AD) (1). BACE1 is a single-membrane spanning protease synthesized in the endoplasmic reticulum and posttranslationally modified by *N*-glycosylation and furin-processing in the Golgi apparatus. Mature BACE1 cycles between the cell surface, endosomes, and trans-Golgi network (TGN) until it ultimately undergoes degradation in the lysosomal compartments. The major determinant in BACE1 sorting to and from endosomes is a short acidic cluster-dileucine motif (DISLL) in its cytosolic tail domain. This motif specifically binds to Golgi-localized  $\gamma$ -ear containing ADP ribosylation factor-binding (GGA-1, GGA-2, and GGA-3) proteins via their Vps, Hrs, and STAM domains (2, 3). GGAs are involved in the selective transport of proteins, including the mannose-6-phosphate receptor, between the TGN and the endosome and in delivering endosomal cargoes for lysosomal degradation (4). Furthermore, in addition to GGA, other proteins, such as reticulons and sorting nexin-6, have been reported to modulate the trafficking of BACE1 (5–7).

The shedding of the major substrate of BACE1, the amyloid precursor protein (APP), appears to occur mainly in early endosomal compartments. Indeed, factors that promote APP or BACE1 internalization (8, 9) enhance  $A\beta$  production, whereas, reversely, blocking their internalization decreases  $A\beta$  levels (10, 11). Although APP contains a cytosolic tyrosine-based NPTY (Asn-Pro-Thr-Tyr) motif (12, 13) and is internalized from the cell

surface to early endosomes through clathrin-dependent endocytosis, the molecular mechanisms of BACE1 internalization and sorting to early endosomal compartments remain to be clarified. BACE1 does not harbor tyrosine-based motifs in its short cytosolic domain, and it is therefore unclear how BACE1 and APP finally end up in the same endosome, where cleavage occurs.

In this study, we identify the small GTPase ADP ribosylation factor 6 (ARF6) as an important modulator of BACE1 sorting. ARF6 is functionally associated with a (subset of) so-called “clathrin/caveolin-independent” endocytic routes (14). These pathways are still somewhat controversial (15), but they can be distinguished on the basis of the involvement of small GTPases, such as cdc42 and RhoA, or by the specific cargo that is transported (e.g., GPI-anchored proteins) (16). Specifically, ARF6 localizes to the plasma membrane and endosomal compartments, where it regulates endocytic trafficking of selective cell surface integral proteins lacking typical clathrin recognition sequences, such as MHC class I (MHCI) proteins and the GPI-anchored CD59 (17, 18). We have now discovered that BACE1 requires ARF6 activity to become sorted to early endosomes, where it encounters APP for processing. Thus, we provide evidence that BACE1 and APP are spatially segregated during plasma membrane-to-early endosome sorting, providing a mechanism for why BACE1 cleaves APP primarily in this compartment. Moreover, this sorting regulation also exists in polarized neurons and, more particularly, in the somatodendritic compartment. The modulation of ARF6 expression ultimately affects  $A\beta$  generation, indicating that interfering with endosomal transport regulation may become an alternative therapeutic strategy for the development of anti-amyloidogenic drugs.

## Results

**APP Shedding by BACE1 Occurs in RAB GTPase 5-Positive Early Endosomes.** To visualize ectodomain shedding of APP, we inserted a cerulean (Cer) (or cherry) fluorescent protein into the ectodomain and fused YFP to the C terminus of APP695 (Fig. 1A). Expression of the Cer-APP-YFP chimera in HeLa cells was confirmed by Western blot analysis displaying both the full-length (FL) fusion protein as well as C-terminal fragments (CTFs), underscoring that Cer-APP-YFP is similarly processed

Author contributions: R.S. and W.A. designed research; R.S., I.D., A.P., T.R., G.M., B.V., and K.C. performed research; G.M., L.Z., S.M., B.D.S., and G.S. contributed new reagents/analytic tools; R.S., I.D., and W.A. analyzed data; and R.S., A.P., T.R., and W.A. wrote the paper.

The authors declare no conflict of interest.

This article is a PNAS Direct Submission.

Freely available online through the PNAS open access option.

<sup>1</sup>To whom correspondence should be addressed. E-mail: wim.annaert@cme.vib-kuleuven.be.

See Author Summary on page 13893.

This article contains supporting information online at [www.pnas.org/lookup/suppl/doi:10.1073/pnas.1100745108/-DCSupplemental](http://www.pnas.org/lookup/suppl/doi:10.1073/pnas.1100745108/-DCSupplemental).

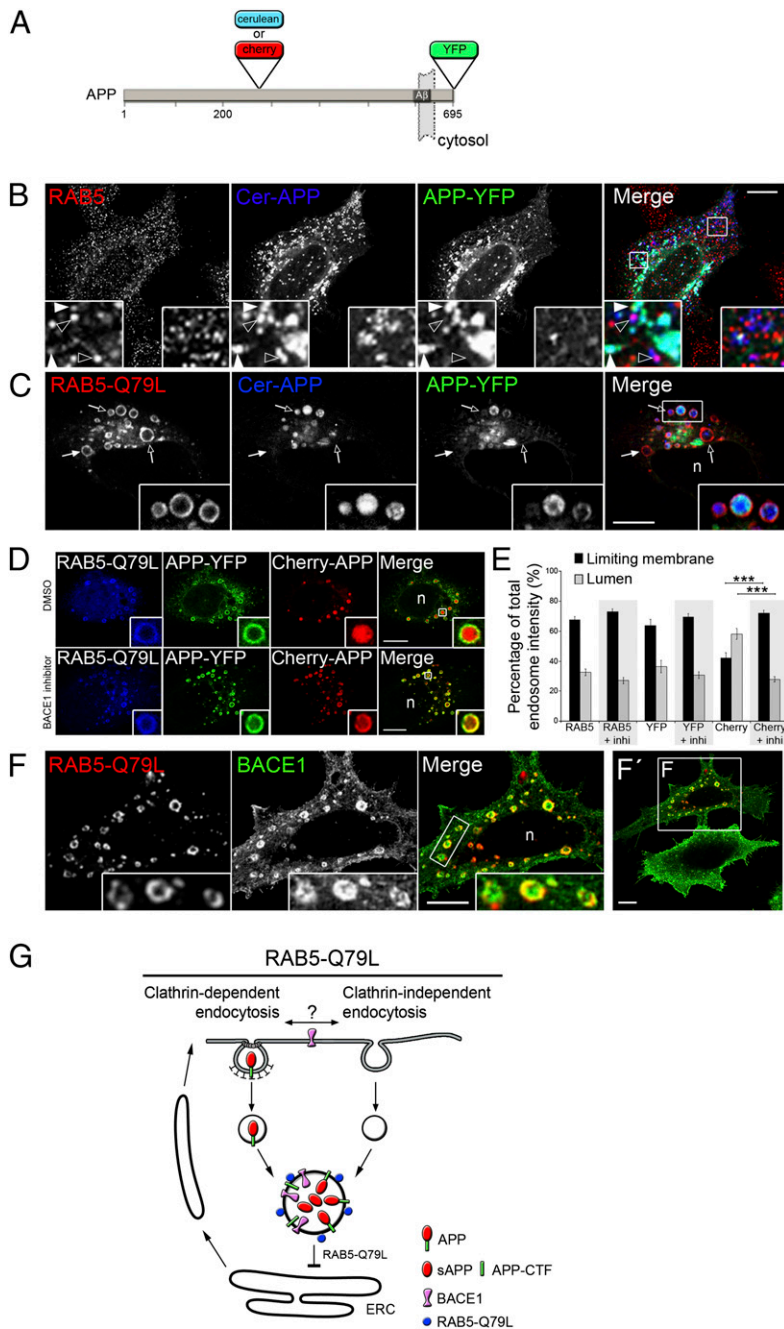


**Fig. 1.** BACE1 cleaves APP within RAB5-positive endosomes. (A) Schematic representation of APP showing where the fluorescent proteins (Cer, cherry, and YFP) were inserted into its sequence. Two chimeric proteins were obtained: a Cer-APP-YFP and a cherry-APP-YFP. (B) HeLa cells transfected with double-tagged APP (Cer-APP-YFP) were fixed and stained for RAB5. (Left Inset) White arrowheads point to colocalization of FL-APP with RAB5, and empty arrowheads indicate colocalization of sAPP (Cer-APP alone) with RAB5. (Right Inset) Area of the cell where sAPP (Cer-APP) is found in vesicular structures distinct from early endosomes, because they do not colocalize with RAB5, is highlighted. (C) HeLa cells cotransfected with double-tagged APP (Cer-APP-YFP) and cherry-RAB5-Q79L. The white arrow points to enlarged RAB5 endosomes devoid of APP, and the empty arrows indicate endosomes containing only the sAPP fragment (Cer-APP). (Insets) Diversity of RAB5-Q79L-positive endosomes with respect to their contents in APP fragments is highlighted. (D) HeLa cells treated with BACE1 inhibitor (10  $\mu$ M, Lower) or with DMSO as a control (Upper) were cotransfected (under continuous inhibition) 2 h later with Cer-RAB5-Q79L and Cherry-APP-YFP. The following day, cells were fixed and processed for imaging. (Insets) For each condition, a representative enlarged RAB5-endosome highlights that in cells treated with BACE1 inhibitor, sAPP (cherry-APP) does not fill the lumen of the endosomes as in control cells but, instead, remains on the limiting membrane. (E) For each condition, fluorescence intensity in the lumen (white bars) and on the limiting membrane (black bars) of  $\sim$ 30 endosomes was measured for each channel and represented in a graph as the percentage of total endosome intensity. The graph clearly shows the shift of localization for sAPP (cherry panel) from the lumen to the limiting membrane upon BACE1 inhibition. (+inhi, with BACE1 inhibitor;  $***P = 0.000001$ ). (F and F') Cells coexpressing Cer-RAB5-Q79L and BACE1 were fixed and stained for BACE1. (F) Magnified view of the area indicated by a white square in F'. (Scale bars = 10  $\mu$ m.) n, nucleus. (G) Schematic representation of BACE1 and APP transport blockade within the endosomal system in cells expressing RAB5-Q79L. Cells expressing RAB5-Q79L develop enlarged endosomes where APP and BACE1 accumulate and APP cleavage occurs. The internalization route of BACE1 is currently unknown (?). ERC, endosomal recycling compartment.

as WT APP (Fig. S1). When analyzed by confocal microscopy, FL Cer-APP-YFP clustered perinuclearly near the Golgi and in a subset ( $17 \pm 8\%$ ,  $n = 8$ ) of RAB GTPase 5 (RAB5)-positive endosomes (Fig. 1B, Left Insets, white arrows). On the other hand,  $69 \pm 8\%$  of peripheral Cer-APP-YFP colocalized with early endosomes in agreement with Burgos et al. (19), underscoring that the inclusion of two fluorescent proteins does not grossly affect the trafficking of APP. Single Cer fluorescence, representing a shed soluble APP ectodomain fragment (sAPP), was also detected in punctate structures that partially colocalized with RAB5 ( $15 \pm 8\%$ , Fig. 1B, Left Insets, open arrows). This supports the view that ectodomain cleavage of the hybrid Cer-APP-YFP occurs in early endosomes (20). In contrast, YFP fluorescence, representing the APP-CTF was rarely detected in RAB5-positive endosomes ( $5 \pm 4\%$ ). This suggests its rapid turnover by  $\gamma$ -secretase processing (Fig. 1B, Right Insets). To study APP shedding in early endosomes in more detail, we blocked

endosomal trafficking of Cer-APP-YFP by coexpressing RAB5-Q79L. This dominant active mutation keeps RAB5 in its GTP-locked form and blocks endosomal maturation, giving rise to enlarged endosomes (21, 22). Cer-APP-YFP became readily trapped; however, this occurred only in a subset of RAB5-Q79L endosomes (Fig. 1C, white arrows), suggesting a selective targeting of APP from the cell surface to a subpopulation of endosomes, which also underscores the heterogeneity in RAB5-Q79L endosomes (23). Under these conditions, single fluorescent Cer-APP (representing sAPP) was mostly found within the lumen of enlarged endosomes (Fig. 1C, open arrows), whereas APP-YFP (representing APP-CTF) was again either absent or detected weakly in the limiting membrane. Next, we coexpressed Cer-RAB5-Q79L with Cherry-APP-YFP in the absence or presence of a BACE1 inhibitor (Fig. 1D). Blocking BACE1 activity shifted cherry fluorescence (sAPP) from a dominant luminal location to the limiting membrane, where it fully colocalized with YFP and

Cer-RAB5 (enlarged endosomes in Fig. 1D, *Insets* and quantified in Fig. 1E). We confirmed this observation using BACE1<sup>-/-</sup> mouse embryonic fibroblasts (MEFs) (Fig. S2). We next tested the idea of whether sAPP fragments detected in early endosomes could primarily originate from processing of APP at the cell sur-

face, followed by subsequent internalization of the shedded fragment. Using cell surface biotinylation, we could not detect sAPP $\alpha$  or sAPP $\beta$  being associated with the plasma membrane (Fig. S3A). Even when HeLa cells were incubated (24 h) with conditioned medium from HEK293 stably expressing human APP695

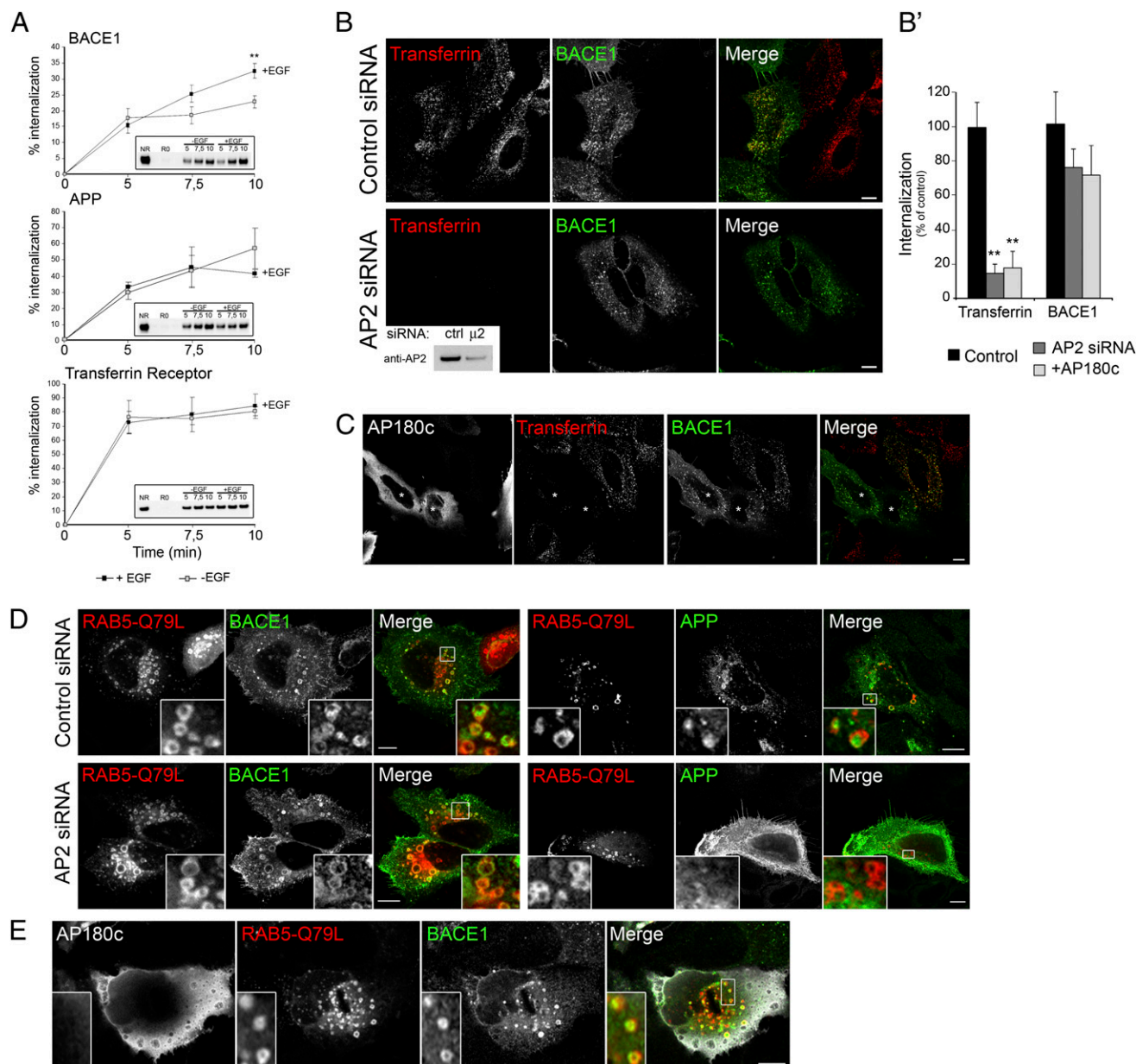


**Fig. 2.** BACE1 internalization is stimulated by EGF and persists when clathrin-mediated internalization is blocked. (A) HEK cells stably expressing APP or BACE1 were starved for 16 h before being subjected to a cell surface biotinylation internalization assay using EZ-Link Sulfo-NHS-SS-Biotin (Pierce) (10 min at 4 °C). After biotinylation, cells were incubated at 37 °C with or without EGF (200 ng/mL) for 5, 7.5, and 10 min, allowing endocytosis to occur. Remaining biotin at the cell surface was cleaved off before cell lysis, and internalized biotinylated proteins were pulled down using streptavidin beads. (*Insets*) Representative Western blots, as well as the mean  $\pm$  SEM ( $n = 3$ ), are shown for BACE1, APP, and TfR. NR, nonreduced sample, R0, reduced sample time point 0. BACE1 antibody uptake in control (nontargeting siRNA) and in AP2 down-regulated ( $\mu$ 2 siRNA) cells (B) or in cells expressing AP180c (C). Cells were incubated on ice with BACE1 antibody (10B8) and Alexa568-labeled transferrin (50  $\mu$ g/mL) and transferred to 37 °C for 20 min to allow internalization. (B) AP2 down-regulation was efficient as shown by Western blot analysis ( $\sim$ 60% down-regulation of total  $\mu$ 2 protein) (*Inset* in B) and by the inhibition of transferrin internalization (*Lower* panel). (C) Anti-myc polyclonal antibody was detected with Alexa647-conjugated secondary antibody. Asterisks indicate cells expressing AP180c. (B') Images for each condition (10–20 cells from 2 experiments) were taken with identical acquisition parameters, and the amount of internalized antibody (10B8) and transferrin was measured and expressed as a percentage of the control condition. Internalization of transferrin was efficiently blocked in AP2 down-regulated cells (\*\* $P = 0.000006$ ) and in cells expressing AP180c (\*\* $P = 0.00006$ ). (D) Twenty-four hours after down-regulation, using  $\mu$ 2 (*Lower*) and control (*Upper*) siRNA, HeLa cells were cotransfected with either BACE1 and Cer-RAB5-Q79L (*Left*) or APP and Cer-RAB5-Q79L (*Right*). The following day, cells were fixed and processed for imaging to detect BACE1 and APP as indicated. (*Insets*) Note that BACE1 is trapped in RAB5-Q79L endosome, whereas APP is accumulating at the cell surface but not in RAB5-Q79L in AP2 down-regulated cells. (E) HeLa cells transfected with AP180c, Cer-RAB5-Q79L, and BACE1 were fixed and processed after 24 h. (*Insets*) Blocking clathrin-dependent endocytosis does not prevent BACE1 from reaching RAB5-Q79L. (Scale bars = 10  $\mu$ m).

and human BACE1 (24) and secreting large amounts of sAPP $\beta$ , no plasma membrane-associated sAPP $\beta$  could be detected with cell surface biotinylation or in the HeLa cell lysate (Fig. S3 B and C). Taken together, all our data strongly seem to support that sAPP accumulating in the lumen of RAB5-Q79L endosomes originates from local BACE1 activity in a subpool of RAB5-positive endosomes. Moreover, by using a BACE1 ectodomain-specific mAb 10B8 in an antibody uptake assay (25), we demonstrate that BACE1 is likely delivered to early endosomes via internalization of its surface-associated pool (Fig. 1G and Fig. S4).

**BACE1 Internalization Is Primarily Distinct from the Canonical Transferrin Receptor-Mediated Endocytosis.** Interestingly, as opposed to the fast clathrin-mediated endocytosis of APP (10, 26), internalization of BACE1 occurs at a slower bulk flow rate, which can be activated by EGF (9). This is also known to stimulate macropinocytosis, an endocytic route not dependent on clathrin (14, 27, 28). Therefore, we surface-biotinylated BACE1, APP, and transferrin receptor (TfR) and followed their internalization in the presence or absence of EGF (200 ng/mL). First, the kinetics of internalization were distinct, with only 20% of BACE1 being internalized after 10 min, while this reached 60% and 80% for APP and TfR, respectively (Fig. 2A). In addition to its slower rate, internalization of BACE1 was significantly stimulated in the presence of EGF (Fig. 2A, *Upper*), whereas APP and transferrin uptake were

not affected (Fig. 2A, *Middle* and *Lower*). Thus, BACE1 vs. APP and TfR endocytosis clearly harbors distinct features. We next down-regulated the heterotetrameric adaptor protein 2 (AP2) complex required for clathrin-mediated endocytosis using siRNA against its  $\mu$ 2 subunit (Fig. 2B and Fig. S5). AP2 down-regulation almost fully blocked Alexa568-conjugated transferrin uptake (Fig. 2B and quantified in Fig. 2B'). On the contrary, BACE1 internalization was not significantly affected in the same cells. This was confirmed by cell surface biotinylation demonstrating that AP2 deficiency causes TfR and APP, but not BACE1, to accumulate at the cell surface (Fig. S5A and B). Also, when we overexpressed the C-terminal domain (AP180c) of AP180, a nonconventional neuronal adaptor protein of the clathrin pathway to block clathrin-mediated internalization (29), transferrin uptake was efficiently impeded. On the contrary, as for AP2 down-regulation, AP180c overexpression largely left BACE1 internalization unaffected (Fig. 2C and quantified in Fig. 2B'). Noteworthy, in both cases, a decreased BACE1 internalization was observed, although statistically not significant. This suggests that minor leakage to canonical clathrin-mediated routes cannot be excluded (see below). Next, we expressed RAB5-Q79L in AP2 down-regulated cells; here, BACE1 was still capable of reaching the enlarged endosomes in contrast to APP, which requires clathrin/AP2 for internalization (26), and therefore remained at the cell surface (Fig. 2D). Expressing AP180c also did not block transport of BACE1 to RAB5-Q79L endosomes

**Fig. 3.** BACE1 cointernalizes with ARF6-cargo molecules CD59 and MHC1. Internalization of surface localized APP (A) and BACE1 (B) in combination with CD59 in HeLa cells was performed 24 h after transfection. Antibody labeling at 4 °C was followed by a 10-min chase at 37 °C in the presence of EGF (200 ng/mL). Following fixation and before permeabilization, cells were incubated with Pacific blue-labeled secondary antibody to visualize the antibodies left at the cell surface; after permeabilization, Alexa488- and Alexa568-labeled secondary antibodies were used to immunolocalize internalized primary antibodies of APP (A) or BACE1 (B) and CD59 (A and B). (A and B, *Right*) Magnifications of selected areas indicated by a square in the merged image; open arrowheads indicate colocalization of BACE1 and CD59. (C) Regions of interest were drawn inside the cells to remove the signal coming from the cell surface, and quantification of colocalization between APP and BACE1 with CD59 was measured and represented as a graph. (D–F) Internalization of surface-localized APP (D) and BACE1 (E) in combination with MHC1 in HeLa cells was performed 24 h after transfection by directly incubating the cells with the antibodies at 37 °C. Ten minutes later, the cells were processed for immunostaining as for A and B, with an additional incubation with the primary antibody against EEA1. This primary antibody was labeled with Alex647 secondary antibody. Magnification of an area indicated by a square in the merge panels in D and E is shown in D' and E'. An additional magnified view from an area in E (upper square in merge panels) is shown in F to indicate the presence of a tubular structure positive for BACE1 and MHC1 (open arrowheads). (G) Images (10–20 cells from 2 experiments) were taken with identical acquisition parameters, and the percentage of MHC1-positive vesicle containing APP or BACE1 is shown in the graph (mean  $\pm$  SD).

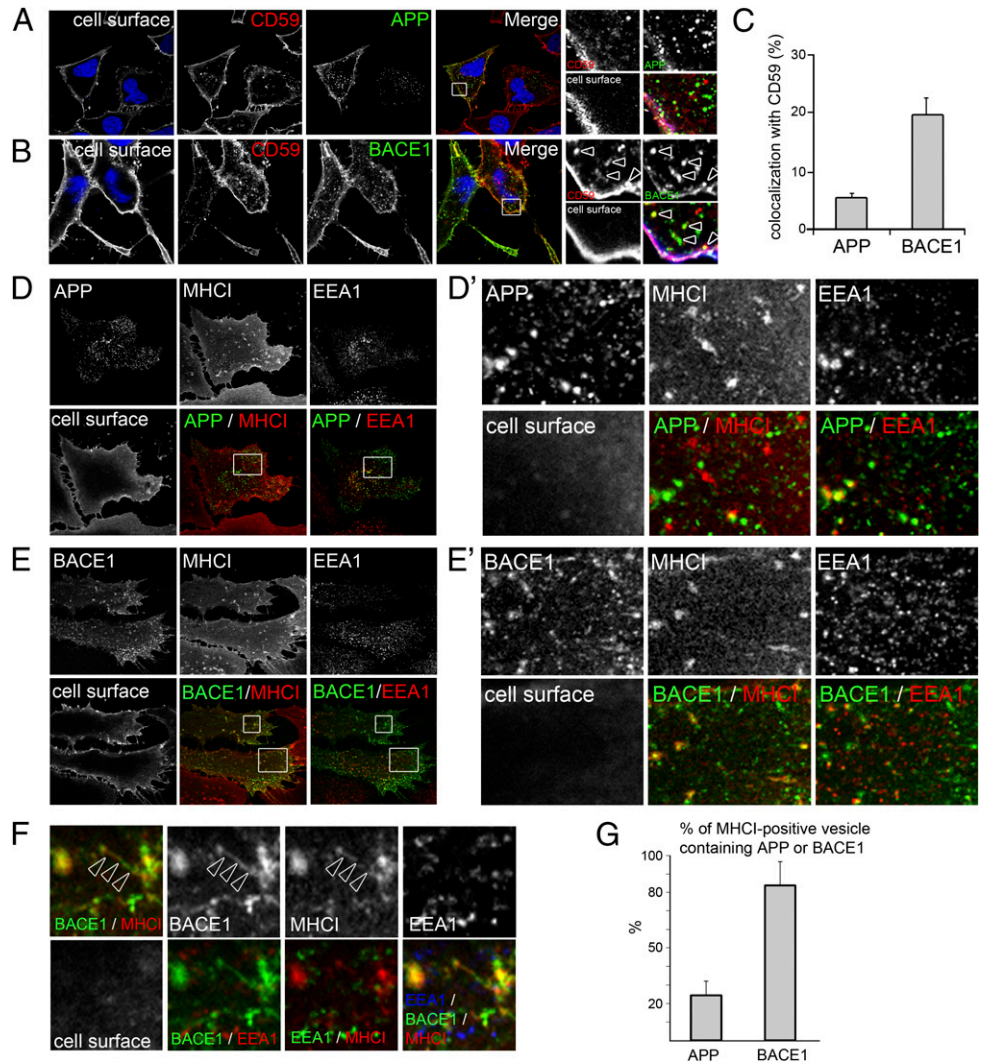


(Fig. 2E, *Insets*). By using independent strategies, our data strongly imply that APP and BACE1 use primarily different routes to become endocytosed and that both pathways can be differentially regulated.

#### BACE1 Follows the Same Internalization Itinerary as CD59 and MHCI.

We next compared the internalization of cell surface-localized BACE1 with CD59, a GPI-anchored cargo protein that has been shown to use a nonclathrin-mediated pathway for its internalization (14, 17). Using a pulse-chase uptake assay with antibodies directed against BACE1 and CD59, a significant portion of the internalized BACE1 colocalized with CD59-positive endosomal compartments. An identical approach analyzing internalized APP and CD59 did not reveal much overlap (Fig. 3A and B, *Insets* and quantified in Fig. 3C). Control experiments in which cells were kept at 4 °C did not show any internalized antibodies (Fig. S6). We next compared the internalization of surface-localized MHCI with either APP or BACE1 following a 10-min uptake at 37 °C (17) (Fig. 3D–G). In this experiment, we additionally immunolocalized Early Endosome Antigen 1 (EEA1) to identify internalized MHCI that has already reached the early endosomal compartment (18). After 10 min of internalization,  $84 \pm 12\%$  ( $n = 12$ ) of MHCI-positive endosomes also contained internalized BACE1 (Fig. 3E, E', and G). Of these, only  $8 \pm 1\%$  were positive for EEA1. On the contrary, only  $25 \pm 8\%$  ( $n = 10$ ) of MHCI-positive endosomes included internalized APP, but almost all ( $93 \pm 7\%$ ) were positive for EEA1 (Fig. 3D, D', and G). Thus, MHCI colocalized with APP when MHCI had already reached the EEA1-positive early endosome (Fig. 3D–G). However, the bulk of internalized MHCI and BACE1 remained negative for EEA1, indicating that they still reside in a distinct endosomal population. In this compartment, MHCI and BACE1 sometimes are colocalized in tubular structures (Fig. 3F, arrowheads) in agreement with the findings of Naslavsky et al. (17).

Endocytic sorting and recycling of CD59 and MHCI are mediated by the small GTPase ARF6 (14). We therefore expressed ARF6-Q67L, an ARF6 mutant locked in its GTP-bound state, to evaluate the effect on BACE1 and APP sorting. Grape-like clusters of vacuoles, characteristic of a blockade in sorting of ARF6-cargo on the way to early endosomes, were observed (17,

30, 31), in which BACE1 became trapped together with known ARF6-cargo molecules, such as MHCI (Fig. 4A). In contrast, APP could not be detected in these ARF6-Q67L vacuoles regardless of whether APP was cotransfected with ARF6-Q67L (Fig. 4B) or in combination with BACE1 and ARF6-Q67L (Fig. 4C).

To demonstrate that ARF6-Q67L expression prevents BACE1 from reaching RAB5-positive endosomes, we coexpressed BACE1 together with ARF6-Q67L and RAB5-Q79L. In contrast to RAB5-Q79L expression alone (Fig. 1F), BACE1 did not accumulate in RAB5-Q79L enlarged endosomes but remained trapped in ARF6-Q67L vacuoles (Fig. 4D), further underscoring the requirement of ARF6 in sorting BACE1, but not APP to early endosomes.

#### Modulation of BACE1 Sorting Through ARF6 Activity Affects APP Processing.

Because ARF6-Q67L blocks the delivery of BACE1 to early endosomes, this implies that GTP hydrolysis of ARF6 is required for the sorting of BACE1 from the preendosomal ARF6 compartment to early endosomes. Hence, we wondered whether we could regulate APP processing via this molecular mechanism. In a first series of experiments, we analyzed the generation of APP carboxyterminal fragments using quantitative Western blotting. ARF6-Q67L expression indeed caused a significant decrease of nearly 50% ( $P < 0.001$ ) in the APP-CTF/FL-APP ratio compared with WT ARF6 (Fig. 5A). Next, we used metabolic labeling to evaluate more quantitatively the effects of WT vs. mutant ARF6 on APP processing. For these experiments, we used SwedishAPP (APP<sup>sw</sup>), a familial AD-linked APP mutant that is more prone to BACE1 processing (32). ARF6-Q67L coexpression dramatically decreased the levels of sAPP-secreted fragments and A $\beta$  peptides, showing that ARF6-Q67L interferes with the normal BACE1 processing of APP. Overactivating endogenous ARF6 by expressing EFA6A, a specific guanine exchange factor (GEF) of ARF6 (33), also significantly decreased A $\beta$  secretion (Fig. S7). ARF6-T27N, a GDP-locked mutant of ARF6, had the reverse effect on APP<sup>sw</sup> processing, resulting in more secreted sAPP and A $\beta$  compared with WT ARF6 (Fig. 5B). In agreement with this, BACE1 and APP were found to accumulate in ARF6-T27N-positive compartments (Fig. 5C and D, *Insets*), providing a possible explanation for the stimulating effects of ARF6-T27N on APP processing. Finally, we studied

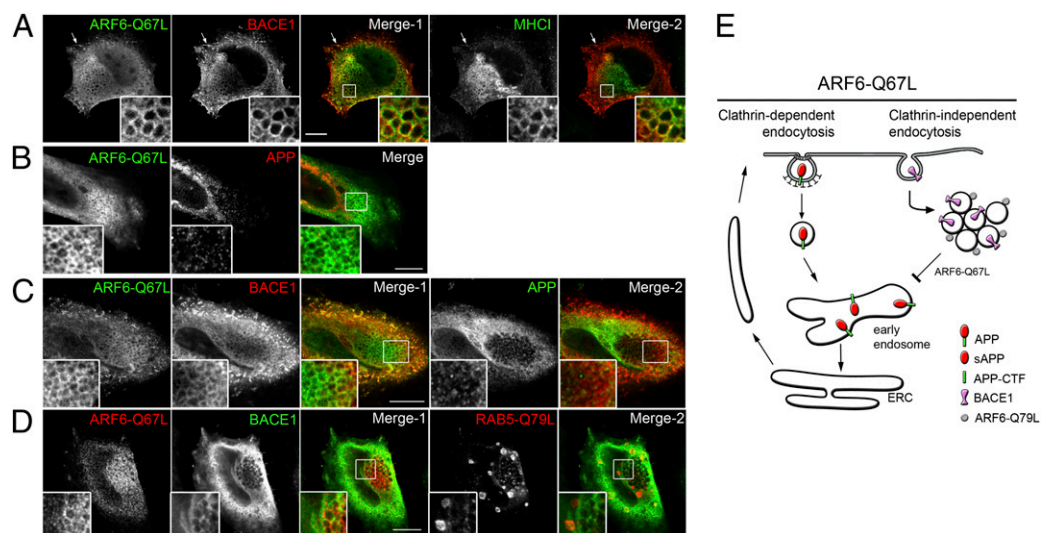


**Fig. 4.** BACE1, unlike APP, is trapped in ARF6-Q67L vacuoles. HeLa cells cotransfected with HA-ARF6-Q67L together with BACE1 (A) or APP (B) or with BACE1 and APP (C) were fixed after 24 h and immunostained for HA, BACE1, APP, and MHCI (A) as indicated. (A and C) BACE1 is present in the ARF6-Q67L vacuoles together with MHCI (A), an ARF6-cargo protein. (B and C) APP is absent from ARF6-positive vacuoles. (*Insets*) Magnified regions are indicated by a square in the merged image. (D) HeLa cells were cotransfected with Cer-RAB5-Q79L, HA-tagged ARF6-Q67L, and BACE1 and fixed after 24 h; they were then stained using antibodies against HA and BACE1. (*Insets*) BACE1 being blocked in ARF6-Q67L vacuoles, is unable to reach RAB5-enlarged endosomes. (Scale bars = 10  $\mu\text{m}$ .) (E) Schematic representation of BACE1 and APP transport blockade within the endosomal system in cells expressing ARF6-Q67L. Expression of ARF6-Q67L blocks the transport and fusion of ARF6 vesicles with early endosomes, resulting in the accumulation of grape-like vacuoles in which BACE1 becomes trapped and thus unable to reach RAB5-positive endosomes. ERC, endosomal recycling compartment.

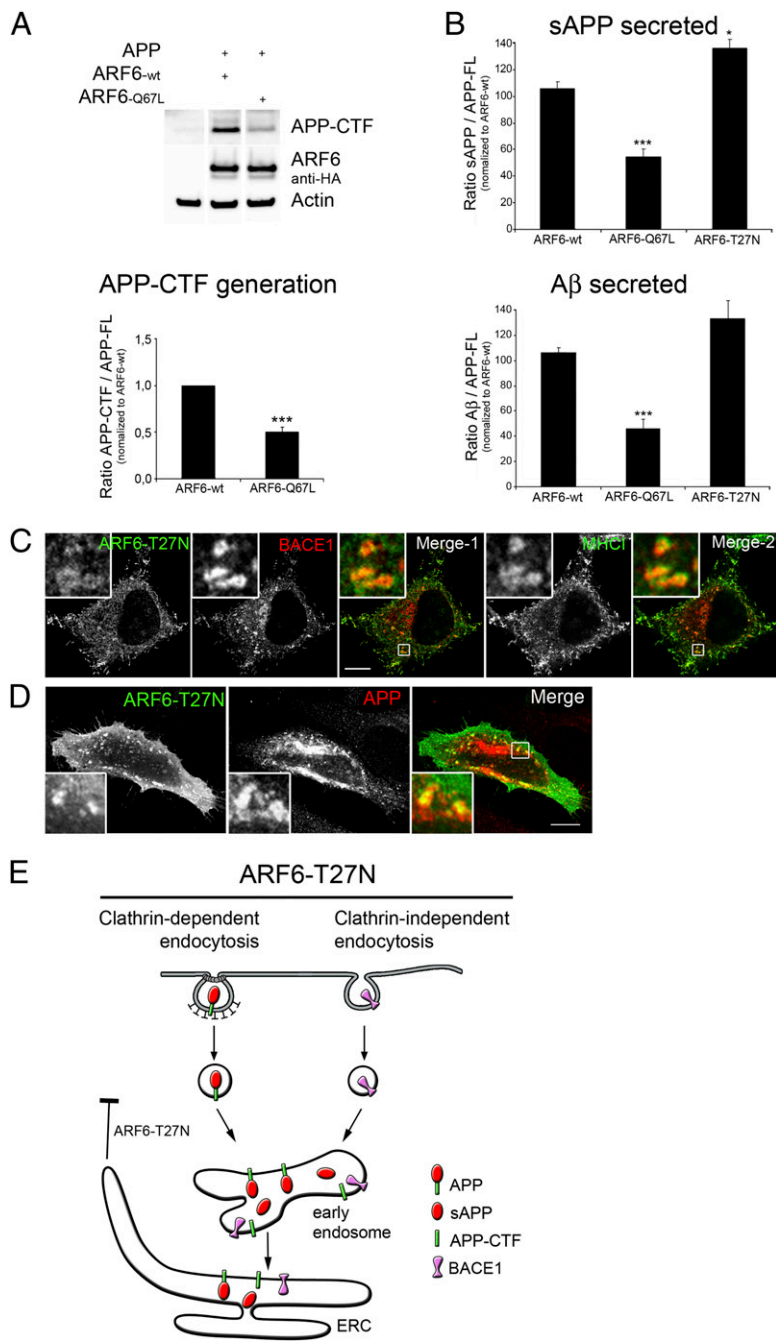


**Fig. 5.** APP processing is affected by expressing dominant ARF6 mutants. (A) HeLa cells cotransfected with APP, WT ARF6, and ARF6-Q67L were lysed. (Upper) Total protein (20  $\mu$ g per lane) was analyzed by Western blot. (Lower) Ratio of APP-CTF over FL-APP was quantified to evaluate the effect of the ARF6-Q67L form (mean  $\pm$  SEM,  $n = 5$ ; Student  $t$  test,  $***P = 0.0007$ ). ARF6-wt, WT ARF6. (B) HeLa cells were cotransfected with APPsw and WT ARF6, ARF6-Q67L, or ARF6-T27N and metabolically labeled. For each experiment, the ratio of sAPP/FL-APP (Upper) and A $\beta$ /FL-APP (Lower) was normalized to WT ARF6 and represented as the mean  $\pm$  SEM [ $n = 3$ , Student  $t$  test: ARF6-Q67L,  $***P = 0.0008$ , and ARF6-T27N,  $*P = 0.022$  (Upper); ARF6-Q67L,  $***P = 0.0001$  (Lower)]. (C) HeLa cells coexpressing HA-tagged ARF6-T27N with either BACE1 (C) or APP (D) were fixed and immunostained for HA, BACE1, MHC1, or APP, as indicated. (Insets) Perinuclear region where BACE1 (C) and APP (D) accumulate within the ARF6-T27N recycling compartment [ $25 \pm 5\%$  of BACE1 and  $32 \pm 12\%$  of APP colocalized with MHC1 ( $\pm$ SD),  $n = 10$ ] is highlighted. (Scale bars = 10  $\mu$ m.) (E) Schematic representation of BACE1 and APP transport blockade within the endosomal system in cells expressing ARF6-T27N. Blocking ARF6-dependent recycling using the ARF6-T27N mutant allows BACE1 and APP to accumulate in the endosomal recycling compartment, thus promoting APP processing. ERC, endosomal recycling compartment.

the effect of long-term ARF6 down-regulation on APP processing. We transfected mouse embryonic fibroblasts (MEFs) with a lentiviral vector harboring an shRNA against murine ARF6 and subsequently generated stable knockdown clones in which ARF6 was down-regulated to almost 90% (ARF6KD MEFs, Fig. S8B, Left). Next, and again using lentiviral technology, we stably expressed human APP695 in control and ARF6KD MEFs and performed metabolic labeling to investigate APP processing. Stable knockdown of ARF6 promoted the production and secretion of sAPP, and A $\beta$  was enhanced compared with WT MEFs (Fig. S8C). Interestingly, the total level of BACE1 in ARF6KD MEFs was increased three-fold, likely explaining the observed enhanced shedding. Surprisingly, BACE1 was only moderately increased at the cell surface (Fig. S8A and B), indicating that a block in internalization could not account for the raised BACE1 levels. In agreement, in ARF6KD MEFs expressing RAB5-Q79L, BACE1 still reached the RAB5-positive

enlarged endosomes (Fig. S8D). In conclusion, both overexpression of ARF6 mutants and stable ARF6 depletion significantly affect APP processing but in opposite ways.

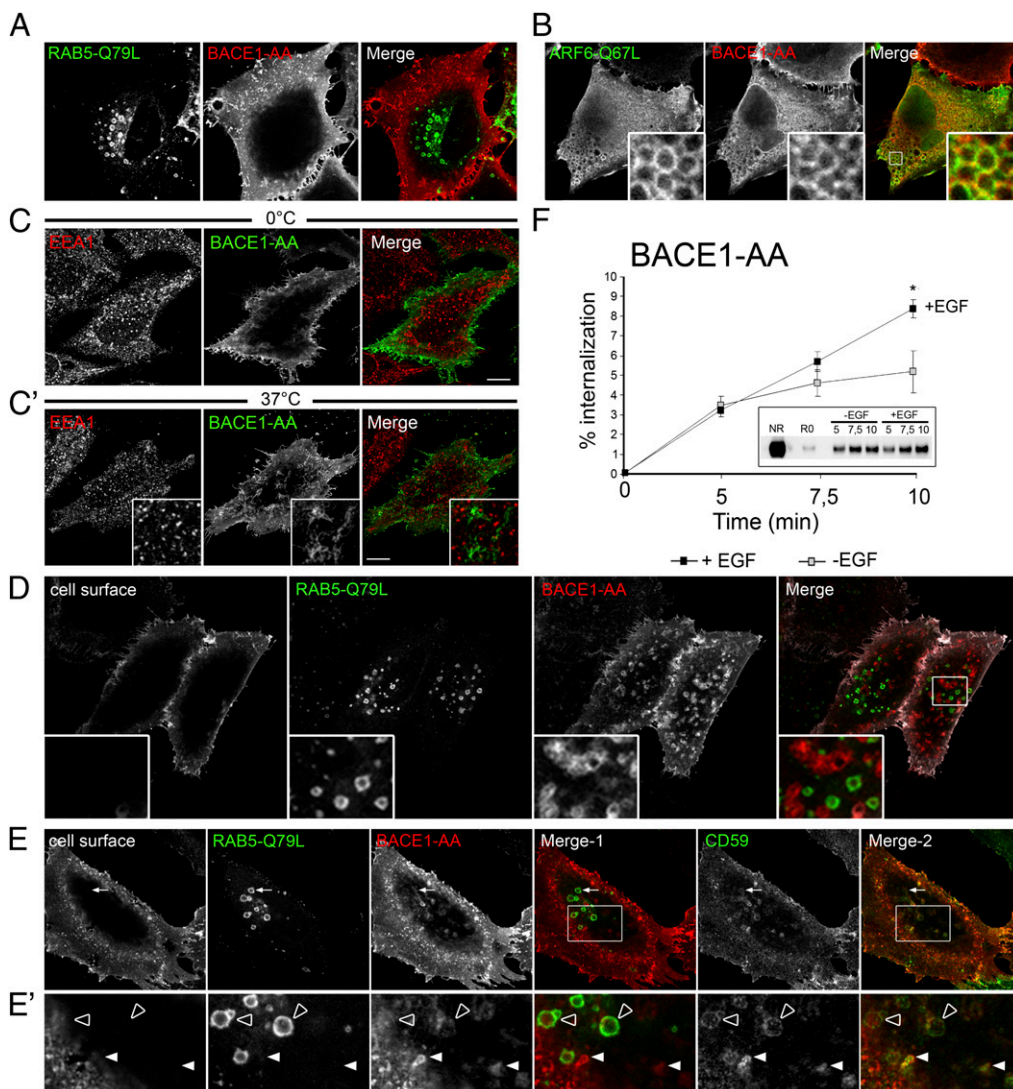
**Sorting of BACE1 to Early Endosomes Is Dependent on the Dileucine Motif.** It has been demonstrated previously that the dileucine motif (DISLLK) in the BACE1 carboxyterminal tail determines, to a significant degree, the localization and trafficking of BACE1 (34–36). This dileucine motif mediates the interaction with GGA proteins (2, 3), and among these, GGA3 is indeed involved in macropinocytotic uptake of ARF6-dependent cargo (33). In agreement with this, we could colocalize some GGA3 with BACE1 (Fig. S9A). However, expressing TBC1D3, a Tre-2/Bub2/Cdc16 (TBC)-containing protein that stimulates macropinocytosis through activation of the ARF6 route and recruitment of GGA3 (33), enhanced the colocalization of GGA3 and BACE1 (Fig. S9B). We therefore mutated both leucines into alanines

(BACE1-AA) to investigate whether this motif was also involved in targeting BACE1 to the early endosomes. BACE1-AA indeed failed to reach RAB5-Q79L enlarged endosomes (Fig. 6A). In contrast, when coexpressed with ARF6-Q67L, BACE1-AA became sequestered to ARF6-Q67L-positive vacuoles (Fig. 6B). Moreover, using antibody uptake experiments, we showed that internalized BACE1-AA-bound antibodies localized to tubular-like structures closely apposed to the cell surface but clearly distinct from EEA1-positive early endosomes (Fig. 6C and C'). In agreement, when the same antibody uptake was done in cells coexpressing RAB5-Q79L, newly internalized BACE1-AA again did not reach RAB5-Q79L endosomes (Fig. 6D-E'). Instead, it colocalized with endocytosed CD59 within similar distinct structures juxtaposed to the cell surface (Fig. 6E and E', white arrowheads). An independent approach using cell surface biotinylation combined with internalization confirmed that BACE1-AA is still endocytosed and remains responsive to EGF (Fig. 6F). The lower extent of internalized BACE1-AA could be explained by the high recycling kinetics of this mutant to the surface as demonstrated by Huse et al. (35). Hence, the structures positive for newly internalized BACE1-AA and CD59 but lacking EEA1 may correspond to the same endocytic compartment that governs the rapid recycling of CD147 (18). Taken together, these data

demonstrate that the dileucine motif is required for sorting of BACE1 from a transient preendosomal compartment to early endosomes, possibly through ARF6 effector molecules.

**BACE1 and APP Processing Is Largely Confined to Somatodendritic Compartments in Polarized Neurons.** Thus far, the ARF6-mediated endosomal sorting of BACE1 was studied in nonneuronal cells. To assess whether ARF6 exerts a similar role in the brain, a major site of amyloidogenic processing, we next explored its subcellular localization and that of BACE1 and APP in neurons. In primary polarized hippocampal neurons (30 days in vitro), endogenous BACE1 and APP immunolocalized predominantly in the somatodendritic compartment based on the codistribution with the dendritic marker MAP2 (Fig. 7A and A'). Likewise, endogenous ARF6 as well as EFA6A, a major GEF for ARF6 in the brain, colocalized in soma and dendrites, whereas they were virtually absent in axons (Fig. 7B and B'). To confirm these findings biochemically, we cultured dorsal root ganglion (DRG) neurons in dual-microfluidic chambers. In the presence of the chemoattractant NGF, axons uniquely grow out through microgrooves into the axonal chamber, physically separating them from soma and dendritic arborization, as shown by tubulin immunostaining (Fig. 7C). Subsequent Western blot analysis of

**Fig. 6.** BACE1-AA fails to reach the RAB5 endosome. HeLa cells coexpressing BACE1-AA with either Cer-RAB5-Q79L (A) or ARF6-Q67L (B) were fixed and immunolabeled for BACE1 and HA. Antibody uptake experiments were performed in cells expressing BACE1-AA alone (C and C', 10 min at 0°C or 37°C, respectively) or with RAB5-Q79L (D-E', 20 min at 37°C), using mAb 10B8 (anti-BACE1) alone (C-D) or with CD59 antibody (E and E'). (C and C') Cells were fixed on ice, permeabilized, and stained for EEA1. (Insets) Tubular-like structures positive for newly internalized BACE1-AA are highlighted. (D-E') Before permeabilization, cells were incubated with Pacific blue-labeled secondary antibody to visualize the remaining primary antibody at the cell surface. After permeabilization, Alexa488- and Alexa568-labeled secondary antibodies were used to localize internalized primary antibodies bound to BACE1 (D-E') and CD59 (E and E'), respectively. (E') Magnified area is indicated by a rectangle in the merge images. White arrowheads indicate colocalization of newly internalized BACE1-AA and CD59, and open arrowheads point to enlarged RAB5-Q79L endosomes containing internalized CD59 but devoid of BACE1-AA. (Scale bars = 10  $\mu$ m.) (F) EGF stimulates BACE1-AA internalization. HEK cells stably expressing BACE1-AA were starved for 16 h before being processed for cell surface biotinylation using EZ-Link Sulfo-NHS-S5-Biotin (Pierce) (10 min at 4°C). After biotinylation, cells were incubated at 37°C without or with EGF (200 ng/mL) for 5, 7.5, and 10 min, allowing endocytosis. The remaining biotin at the cell surface was cleaved off before cell lysis, and internalized biotinylated proteins were pulled down using streptavidin beads. (Insets) Representative Western blot and mean  $\pm$  SEM of the percentage of internalized BACE1-AA of three independent experiments are shown.



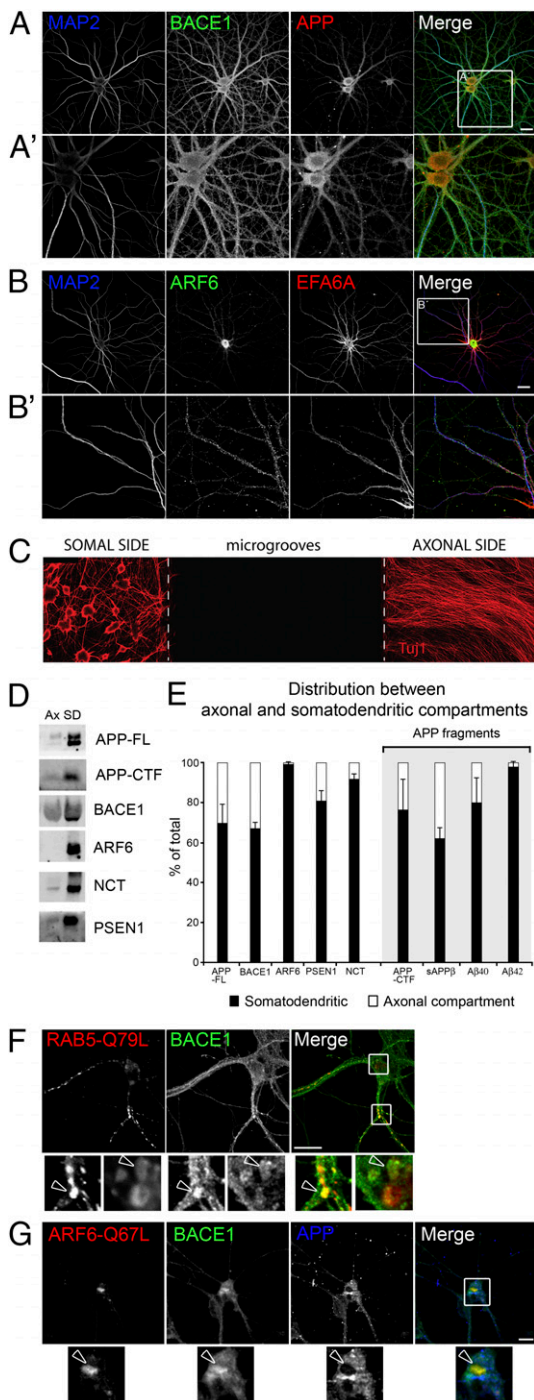


**Fig. 7.** BACE1, APP, and ARF6 are largely present in the somatodendritic compartment in polarized neurons. (A) Rat hippocampal neurons were cultured for 4 wk in vitro, fixed, and stained with anti-MAP2 antibody (blue) to reveal dendrites, anti-BACE1 antibody (10B8, green), and anti-APP antibody (C-terminal, red), and were subsequently analyzed by confocal microscopy. (A') Higher magnification shows BACE1 evidently localizing to the soma, dendrites, and axon. APP distribution is more confined to the cell body and dendrites. (B) Rat hippocampal neurons were cultured for 2 wk in vitro, fixed, and stained with anti-MAP2 (blue) to reveal dendrites, anti-ARF6 antibody (3A-1, green), anti-EFA6A (polyclonal antibody 1626, red), and analyzed by confocal microscopy. (B') Higher magnification shows EFA6A and ARF6 predominantly localizing to the somatodendritic compartment. (C) DRG neurons were cultured for 7 d in chambers containing microgrooves to separate axons physically from the somatodendritic compartment. These neurons were fixed and stained with anti-Tuj1 (antibody against  $\beta$ -Tubulin III, red). (D) Western blot analysis of extracts derived from the somatodendritic or axonal lysates corroborated the abundant localization of APP and BACE1 in the somatodendritic compartment (Fig. 7D and quantified in Fig. 7E). Analysis of the conditioned media showed that  $62 \pm 6\%$  of sAPP $\beta$  is secreted in the somatodendritic chamber. Interestingly, up to  $80 \pm 12\%$  of A $\beta$ 40 and almost all A $\beta$ 42 ( $98 \pm 4\%$ ) was recovered here in agreement with an equal predominant localization of presenilin 1 and nicastrin, two integral components of the  $\gamma$ -secretase complex, in soma and dendrites. Interestingly, the low axonal levels of APP, BACE1, and both  $\gamma$ -secretase components surprisingly match the relative amounts of the respective processed fragments, sAPP $\beta$  and A $\beta$ , recovered in the conditioned axonal medium (Fig. 7E). Furthermore, virtually no endogenous ARF6 was detected in axons ( $<1\%$  of total), suggesting that BACE1 endosomal sorting may be differently regulated here, whereas the major pool of BACE1 in soma and dendrites is more controlled through ARF6. In agreement, when ARF6-Q67L was overexpressed in primary hippocampal neurons, endogenous BACE1 but not APP was trapped in somatically localized ARF6-positive vacuoles (Fig. 7G). Similarly, RAB5-Q79L enlarged endosomes were only found in soma and dendrites and were often BACE1-positive (Fig. 7F, Insets, arrowheads). Overall, we can conclude that major amyloidogenic processing of APP in primary neurons is confined to the somatodendritic compartment.

the cell/axonal lysates corroborated the abundant localization of APP and BACE1 in the somatodendritic compartment (Fig. 7D and quantified in Fig. 7E). Analysis of the conditioned media showed that  $62 \pm 6\%$  of sAPP $\beta$  is secreted in the somatodendritic chamber. Interestingly, up to  $80 \pm 12\%$  of A $\beta$ 40 and almost all A $\beta$ 42 ( $98 \pm 4\%$ ) was recovered here in agreement with an equal predominant localization of presenilin 1 and nicastrin, two integral components of the  $\gamma$ -secretase complex, in soma and dendrites. Interestingly, the low axonal levels of APP, BACE1, and both  $\gamma$ -secretase components surprisingly match the relative amounts of the respective processed fragments, sAPP $\beta$  and A $\beta$ , recovered in the conditioned axonal medium (Fig. 7E). Furthermore, virtually no endogenous ARF6 was detected in axons ( $<1\%$  of total), suggesting that BACE1 endosomal sorting may be differently regulated here, whereas the major pool of BACE1 in soma and dendrites is more controlled through ARF6. In agreement, when ARF6-Q67L was overexpressed in primary hippocampal neurons, endogenous BACE1 but not APP was trapped in somatically localized ARF6-positive vacuoles (Fig. 7G). Similarly, RAB5-Q79L enlarged endosomes were only found in soma and dendrites and were often BACE1-positive (Fig. 7F, Insets, arrowheads). Overall, we can conclude that major amyloidogenic processing of APP in primary neurons is confined to the somatodendritic compartment.

### Discussion

Our study conclusively demonstrates that the sorting of BACE1 to endosomes is primarily controlled by the small GTPase ARF6, reminiscent of other cargo proteins like CD59 and MHCI, and largely persists when clathrin-dependent endocytosis is inhibited. Furthermore, the slow internalization kinetics of BACE1 and sensitivity to EGF stimulation, not observed for clathrin-mediated endosomal cargo like APP and TfR, add to the overall conclusion that endocytosis and endocytic sorting of BACE1 and APP are distinctly regulated (Fig. 8). Consequently, interfering with just one mechanism, as we demonstrate by modulating ARF6 activity, is sufficient to alter APP processing and A $\beta$  production significantly. For instance, expressing dominant active ARF6-Q67L prevented internalized BACE1 from reaching RAB5-positive endosomes, hence precluding it from accessing its substrate APP for processing (Fig. 4E).

Moreover, our findings strengthen the central role of the dileucine motif within the BACE1 intracellular domain in the main transport routes of BACE1 to endosomes. Indeed, it has already been demonstrated that BACE1 is targeted from the TGN directly to endosomes through selective interactions of this motif with the three GGA proteins (2, 3). From there, BACE1 can recycle back or traffic to the cell surface. Plasma membrane-

driftic or axonal compartment of the DRG cultures (*Materials and Methods*). Ax, axonal; SD, somatodendritic. (E) Signal intensities were measured (3 independent experiments), and the percentage of distribution of each protein was calculated and is shown. A quantitative analysis of the distribution of BACE1, APP, and other components in the axonal or somatodendritic compartment derived from the DRG cultures is shown. In addition to quantifications derived from the Western blot analysis, the chart indicates the extent to which the different APP fragments (APP-CTF, sAPP $\beta$ , A $\beta$ 40, and A $\beta$ 42) are polarized (gray background). Secreted sAPP $\beta$  was quantified after immunoprecipitation and Western blot analysis, whereas secreted A $\beta$ 40 and A $\beta$ 42 were quantified using ELISA (*Materials and Methods*). Rat hippocampal neurons were cultured for 11 d in vitro and subsequently transfected with either Cer-tagged RAB5-Q79L (F) or HA-tagged ARF6-Q67L (G). Cells were fixed at 36 h posttransfection and stained with anti-BACE1 (10B8, green) (F and G) or anti-APP (C-terminal, blue) and anti-HA (for ARF6-Q67L) (G), and they were subsequently analyzed by confocal microscopy. Higher magnification shows accumulation of BACE1 in enlarged RAB5-Q79L endosomes along dendrites and in the soma (F, Insets, open arrowheads) or in ARF6-Q67L vacuoles (G, Insets, open arrowheads). In contrast to APP, BACE1 evidently gets trapped in ARF6-Q67L-positive structures, which are also primarily found at the cell body. (Scale bar = 10  $\mu$ m.)

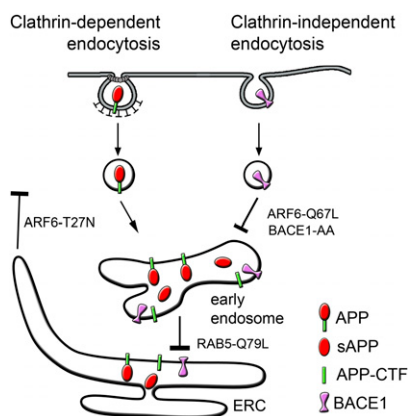


**Fig. 8.** Distinct transport itineraries of BACE1 and APP to early endosomes. Schematic overview represents the effect of the distinct endosomal blocking mutants on BACE1 and APP trafficking. BACE1 and APP efficiently accumulate in RAB5-Q79L endosomes. ARF6-Q67L expression traps BACE1 and prevents its delivery to RAB5-positive endosomes, and thereby inhibits APP processing. ARF6-T27N expression blocks recycling from the endosomal recycling compartment to the cell surface, which allows APP to be processed efficiently by BACE1. Note that BACE1-AA likely blocks the transport between ARF6 vesicles and early endosomes. ERC, endosomal recycling compartment.

to-early endosome sorting also requires the dileucine motif, however, likely at the step following internalization. Indeed, internalized BACE1-AA is not capable of reaching RAB5-positive early endosomes, fostering our conclusion that the dileucine motif mediates the sorting of internalized BACE1 from pre-sorting endosomal structures to early endosomes (this study and ref. 35). The existence of such an intermediate between the plasma membrane and early endosomes is reminiscent of CD59, another cargo molecule whose endosomal transport is mediated through ARF6 activity (37). Based on our observation that GGA3 more prominently colocalizes with BACE1 in membrane ruffles in TBC1D3-overexpressing cells, we can speculate that GGA3 functions as an ARF6 effector in this transport regulation to early endosomes. With respect to APP, it was shown recently to interact with the AP4 adaptor complex at the TGN (19), supporting that APP and BACE1 trafficking is differently regulated at the site of TGN exit. Also, once APP arrives at the cell surface, it reinternalizes differently from BACE1 (i.e., via a well-characterized tyrosine-based motif that mediates its endocytosis in a clathrin-, AP2-, dynamin-dependent manner) (Fig. 8) (13, 26). Further differences are also found at the level of microdomain association of BACE1 and APP, which could mechanistically underlay distinct sorting requirements. Although both proteins fractionate to cholesterol-rich domains (38, 39), they were shown to be present in distinct microdomains (40, 41). Furthermore, APP is able to shift to the BACE1-associated microdomain after phosphorylation of Munc18, an APP-binding protein (41). Interestingly, cross-linking these distinct microdomains is not sufficient to promote APP processing but required an additional endocytic step (40). This agrees well with the fact that APP and BACE1 follow distinct internalization routes to a common early endosome (Fig. 8) and that BACE1 processing is optimal in more acidic environments (42, 43). Moreover, our data may suggest that the dynamic exchange of APP and BACE1 between distinct microdomains, as observed by Sakurai et al. (41), could occur at the level of the early endosomes. If so, this further emphasizes the role of the early endosome as a signaling compartment (44, 45) where major APP processing is initiated, thereby abrogating its function or initiating downstream signaling (46, 47).

From a general physiological perspective, the ARF6-dependent routes are gaining increasing attention by cell biologists. A major reason is that the cell/neuron may use the constitutive

or stimulated ARF6 routes to control directly or indirectly the steady-state levels of cell surface receptors important for signaling, as described, for instance, for the EGF receptor (48, 49), migration, or antigen presentation (50–52). Similarly, the ARF6 route likely indirectly controls APP processing by modulating BACE1 trafficking in neurons. By affecting its processing, ARF6 activity may also modulate the diverse neuronal functions of APP, including migration (53), neurite outgrowth (54), synaptic plasticity (55), and axonal pruning/neuronal death (56). The almost exclusive somatodendritic localization of ARF6 underscores a selective effect on processing in this part of polarized neurons. The extent of ARF6 influence on processing can be significant, because BACE1 and  $\gamma$ -secretase, as well as their secreted products sAPP $\beta$  and A $\beta$ , are most prominently detected in the somatodendritic chamber of a compartmentalized microfluidic culture system. On the other hand, the low levels of APP and BACE1, as well as sAPP $\beta$ , in the axonal compartment in the virtual absence of ARF6, as demonstrated in this study, suggest alternative endosomal sorting regulation in axons.

Abrogating ARF6 function by stable knockdown resulted in significantly higher cellular BACE1 levels and promoted APP processing, including increased A $\beta$  secretion (Fig. S8), strikingly similar to what is observed for GGA3 knockdown (6). Because GGA3 knockdown prevents BACE1 from being degraded (57) and functions as an ARF6 effector (33), this fuels the idea that the ARF6-dependent endosomal transport regulation of BACE1 is affected in both cases. Because GGA3 levels are as well downregulated in the brain of patients with AD (6), these independent findings suggest that not only GGA3 and ARF6 but likely many more effectors of ARF6 can be considered from a therapeutic point of view, with the aim of modulating APP processing through regulating BACE1 transport, recycling, and turnover in endosomes. Because ARF6 has broad cellular functions (58), the therapeutic quest will be to find regulators with a specific spatial distribution and temporal expression pattern that can reduce APP processing and minimally compromise other essential functions of ARF6 (59). The most effective additional targets could be the specific GEFs or GTPase-activating proteins (GAPs) that regulate ARF6 activity or other RAB-GTPases and their effectors in endosomal recycling. For example, EFA6A is an ARF6-GEF highly restricted to brain (60) and localizes (like ARF6) to the somatodendritic compartment in agreement with its role in regulating dendritic spine formation (60, 61). Overexpressing EFA6A indeed affects A $\beta$  secretion (Fig. S7), underscoring our premise that targeting ARF6 effectors could be equally efficient in modulating ARF6-regulated endosomal sorting.

Taken together, we conclusively demonstrate that BACE1 reaches the early endosomal compartment through a mechanism mediated by ARF6, which is principally distinct from the clathrin-dependent route operated by APP (Fig. 8). Our study therefore demonstrates that sorting of BACE1 and APP can be independently regulated, implying that factors or compounds selectively affecting endocytic sorting and recycling of either BACE1 or APP harbor novel and largely unexplored therapeutic potentials relevant for AD.

## Materials and Methods

Detailed methods and materials are provided in *SI Materials and Methods*. Herein, all cell lines, chemicals, antibodies, RNAi and plasmids used in this study are listed as well as details on transfection. For this study MEFs were generated in which ARF6 was stably downregulated using lentiviral shRNA particles including the ARF6 targeting oligo. All confocal microscopy was done on a Radiance2100 (Carl Zeiss microimaging, Inc.) connected to an Eclipse E800 Nikon upright microscope. Quantifications of colocalization were done using Image J software as explained in more detail in *SI Materials and Methods*.

Biochemical analysis includes metabolic labeling and immunoprecipitation, western blotting, cell surface biotinylation, and internalization assays as well as the use of commercial ELISA-kits for A $\beta$  measurements and protein determination.

Primary hippocampal neurons were derived from embryo day E17 or E18 mouse or rat embryos. Dissociated dorsal root ganglion neurons

were obtained from E13.5 mouse embryos and cultured in microfluidic chambers.

**ACKNOWLEDGMENTS.** The authors are indebted to J. Donaldson, H. McMahon, P. Chavrier, S. Confalonieri, M. Zerial, V. Hsu, J. Walter, and C. Haass for providing plasmids and cell lines and to R. Jahn, B. Greenberg, and E. Kim for providing antibodies. We thank W. Vermeire, K. Vennekens, and T. Wahle for technical help and scientific discussions. This work was financially supported

by the Vlaams Instituut voor Biotechnologie (VIB); Grants G.0663.09 and G.0.754.10.N from the Fonds voor Wetenschappelijk Onderzoek; Grant AKUL/09/037 from the Hercules Foundation; Grant SAO-FRMA/2008 from the Stichting Alzheimer Onderzoek; a grant from Methusalem, Catholic University of Leuven (to B.D.S.); Grant IAP P6/43 from the federal government; and Grant IIRG-08-91535 from the Alzheimer Association. T.R. is the holder of a postdoctoral fellowship from the Catholic University of Leuven, and R.S. obtained a Marie-Curie postdoctoral fellowship.

- Vassar R, Kovacs DM, Yan R, Wong PC (2009) The beta-secretase enzyme BACE in health and Alzheimer's disease: Regulation, cell biology, function, and therapeutic potential. *J Neurosci* 29:12787–12794.
- He X, Chang WP, Koelsch G, Tang J (2002) Memapsin 2 (beta-secretase) cytosolic domain binds to the VHS domains of GGA1 and GGA2: Implications on the endocytosis mechanism of memapsin 2. *FEBS Lett* 524:183–187.
- Wahle T, et al. (2005) GGA proteins regulate retrograde transport of BACE1 from endosomes to the trans-Golgi network. *Mol Cell Neurosci* 29:453–461.
- Bonifacino JS (2004) The GGA proteins: Adaptors on the move. *Nat Rev Mol Cell Biol* 5:23–32.
- He W, et al. (2004) Reticulon family members modulate BACE1 activity and amyloid-beta peptide generation. *Nat Med* 10:959–965.
- Tesco G, et al. (2007) Depletion of GGA3 stabilizes BACE and enhances beta-secretase activity. *Neuron* 54:721–737.
- Okada H, et al. (2010) Proteomic identification of sorting nexin 6 as a negative regulator of BACE1-mediated APP processing. *FASEB J* 24:2783–2794.
- Grbovic OM, et al. (2003) Rab5-stimulated up-regulation of the endocytic pathway increases intracellular beta-cleaved amyloid precursor protein carboxyl-terminal fragment levels and Abeta production. *J Biol Chem* 278:31261–31268.
- Zou L, et al. (2007) Receptor tyrosine kinases positively regulate BACE activity and Amyloid-beta production through enhancing BACE internalization. *Cell Res* 17:389–401.
- Carey RM, Balcz BA, Lopez-Coviella I, Slack BE (2005) Inhibition of dynamin-dependent endocytosis increases shedding of the amyloid precursor protein ectodomain and reduces generation of amyloid beta protein. *BMC Cell Biol* 6:30–40.
- Chyung JH, Selkoe DJ (2003) Inhibition of receptor-mediated endocytosis demonstrates generation of amyloid beta-protein at the cell surface. *J Biol Chem* 278:51035–51043.
- Traub LM (2009) Tickets to ride: Selecting cargo for clathrin-regulated internalization. *Nat Rev Mol Cell Biol* 10:583–596.
- Perez RG, et al. (1999) Mutagenesis identifies new signals for beta-amyloid precursor protein endocytosis, turnover, and the generation of secreted fragments, including Abeta42. *J Biol Chem* 274:18851–18856.
- Donaldson JG, Porat-Shliom N, Cohen LA (2009) Clathrin-independent endocytosis: A unique platform for cell signaling and PM remodeling. *Cell Signal* 21:1–6.
- Grant BD, Donaldson JG (2009) Pathways and mechanisms of endocytic recycling. *Nat Rev Mol Cell Biol* 10:597–608.
- Howes MT, et al. (2010) Clathrin-independent carriers form a high capacity endocytic sorting system at the leading edge of migrating cells. *J Cell Biol* 190:675–691.
- Naslavsky N, Weigert R, Donaldson JG (2004) Characterization of a nonclathrin endocytic pathway: membrane cargo and lipid requirements. *Mol Biol Cell* 15:3542–3552.
- Eyster CA, et al. (2009) Discovery of new cargo proteins that enter cells through clathrin-independent endocytosis. *Traffic* 10:590–599.
- Burgos PV, et al. (2010) Sorting of the Alzheimer's disease amyloid precursor protein mediated by the AP-4 complex. *Dev Cell* 18:425–436.
- Rajendran L, et al. (2006) Alzheimer's disease beta-amyloid peptides are released in association with exosomes. *Proc Natl Acad Sci USA* 103:11172–11177.
- Stenmark H, et al. (1994) Inhibition of rab5 GTPase activity stimulates membrane fusion in endocytosis. *EMBO J* 13:1287–1296.
- Rink J, Ghigo E, Kalaidzidis Y, Zerial M (2005) Rab conversion as a mechanism of progression from early to late endosomes. *Cell* 122:735–749.
- Wegner CS, et al. (2010) Ultrastructural characterization of giant endosomes induced by GTPase-deficient Rab5. *Histochem Cell Biol* 133:41–55.
- Walter J, et al. (2001) Phosphorylation regulates intracellular trafficking of beta-secretase. *J Biol Chem* 276:14634–14641.
- Zhou L, et al. (2011) Inhibition of beta-secretase in vivo via antibody binding to unique loops (D and F) of BACE1. *J Biol Chem* 286:8677–8687.
- Schneider A, et al. (2008) Flotillin-dependent clustering of the amyloid precursor protein regulates its endocytosis and amyloidogenic processing in neurons. *J Neurosci* 28:2874–2882.
- Lanzetti L, Palamidessi A, Arecas L, Scita G, Di Fiore PP (2004) Rab5 is a signalling GTPase involved in actin remodelling by receptor tyrosine kinases. *Nature* 429:309–314.
- Mettlen M, et al. (2006) Src triggers circular ruffling and macropinocytosis at the apical surface of polarized MDCK cells. *Traffic* 7:589–603.
- Zhao X, et al. (2001) Expression of auxilin or AP180 inhibits endocytosis by mislocalizing clathrin: Evidence for formation of nascent pits containing AP1 or AP2 but not clathrin. *J Cell Sci* 114:353–365.
- Brown FD, Rozelle AL, Yin HL, Balla T, Donaldson JG (2001) Phosphatidylinositol 4,5-bisphosphate and Arf6-regulated membrane traffic. *J Cell Biol* 154:1007–1017.
- Naslavsky N, Weigert R, Donaldson JG (2003) Convergence of non-clathrin- and clathrin-derived endosomes involves Arf6 inactivation and changes in phosphoinositides. *Mol Biol Cell* 14:417–431.
- Mullan M, et al. (1992) A pathogenic mutation for probable Alzheimer's disease in the APP gene at the N-terminus of beta-amyloid. *Nat Genet* 1:345–347.
- Frittoli E, et al. (2008) The primate-specific protein TBC1D3 is required for optimal macropinocytosis in a novel ARF6-dependent pathway. *Mol Biol Cell* 19:1304–1316.
- Pastorino L, Ikin AF, Nairn AC, Pursnani A, Buxbaum JD (2002) The carboxyl-terminus of BACE contains a sorting signal that regulates BACE trafficking but not the formation of total A(beta). *Mol Cell Neurosci* 19:175–185.
- Huse JT, Pijak DS, Leslie GJ, Lee VM, Doms RW (2000) Maturation and endosomal targeting of beta-site amyloid precursor protein-cleaving enzyme. The Alzheimer's disease beta-secretase. *J Biol Chem* 275:33729–33737.
- Capell A, et al. (2000) Maturation and pro-peptide cleavage of beta-secretase. *J Biol Chem* 275:30849–30854.
- Cai B, Katafiasz D, Horejsi V, Naslavsky N (2011) Pre-sorting endosomal transport of the GPI-anchored protein, CD59, is regulated by EHD1. *Traffic* 12:102–120.
- Vetrivel KS, et al. (2005) Spatial segregation of gamma-secretase and substrates in distinct membrane domains. *J Biol Chem* 280:25892–25900.
- Riddell DR, Christie G, Hussain I, Dingwall C (2001) Compartmentalization of beta-secretase (Asp2) into low-buoyant density, noncaveolar lipid rafts. *Curr Biol* 11:1288–1293.
- Ehehalt R, Keller P, Haass C, Thiele C, Simons K (2003) Amyloidogenic processing of the Alzheimer beta-amyloid precursor protein depends on lipid rafts. *J Cell Biol* 160:113–123.
- Sakurai T, et al. (2008) Membrane microdomain switching: A regulatory mechanism of amyloid precursor protein processing. *J Cell Biol* 183:339–352.
- Lin X, et al. (2000) Human aspartic protease memapsin 2 cleaves the beta-secretase site of beta-amyloid precursor protein. *Proc Natl Acad Sci USA* 97:1456–1460.
- He X, et al. (2003) Biochemical and structural characterization of the interaction of memapsin 2 (beta-secretase) cytosolic domain with the VHS domain of GGA proteins. *Biochemistry* 42:12174–12180.
- Sorkin A, von Zastrow M (2009) Endocytosis and signalling: Intertwining molecular networks. *Nat Rev Mol Cell Biol* 10:609–622.
- Gould GW, Lippincott-Schwartz J (2009) New roles for endosomes: From vesicular carriers to multi-purpose platforms. *Nat Rev Mol Cell Biol* 10:287–292.
- Reinhard C, Hébert SS, De Strooper B (2005) The amyloid-beta precursor protein: Integrating structure with biological function. *EMBO J* 24:3996–4006.
- Thinakaran G, Koo EH (2008) Amyloid precursor protein trafficking, processing, and function. *J Biol Chem* 283:29615–29619.
- Sigismund S, et al. (2008) Clathrin-mediated internalization is essential for sustained EGFR signaling but dispensable for degradation. *Dev Cell* 15:209–219.
- Morishige M, et al. (2008) GEP100 links epidermal growth factor receptor signalling to Arf6 activation to induce breast cancer invasion. *Nat Cell Biol* 10:85–92.
- Balasuubramanian N, Scott DW, Castle JD, Casanova JE, Schwartz MA (2007) Arf6 and microtubules in adhesion-dependent trafficking of lipid rafts. *Nat Cell Biol* 9:1381–1391.
- Sabe H (2003) Requirement for Arf6 in cell adhesion, migration, and cancer cell invasion. *J Biochem* 134:485–489.
- Walseng E, Bakke O, Roche PA (2008) Major histocompatibility complex class II-peptide complexes internalize using a clathrin- and dynamin-independent endocytosis pathway. *J Biol Chem* 283:14717–14727.
- Young-Pearse TL, et al. (2007) A critical function for beta-amyloid precursor protein in neuronal migration revealed by in utero RNA interference. *J Neurosci* 27:14459–14469.
- Young-Pearse TL, Chen AC, Chang R, Marquez C, Selkoe DJ (2008) Secreted APP regulates the function of full-length APP in neurite outgrowth through interaction with integrin beta1. *Neural Dev* 3:15–27.
- Shankar GM, et al. (2008) Amyloid-beta protein dimers isolated directly from Alzheimer's brains impair synaptic plasticity and memory. *Nat Med* 14:837–842.
- Nikolaev A, McLaughlin T, O'Leary DD, Tessier-Lavigne M (2009) APP binds DR6 to trigger axon pruning and neuron death via distinct caspases. *Nature* 457:981–989.
- Kang EL, Cameron AN, Piazza F, Walker KR, Tesco G (2010) Ubiquitin regulates GGA3-mediated degradation of BACE1. *J Biol Chem* 285:24108–24119.
- Schweitzer JK, Sedgwick AE, D'Souza-Schorey C (2011) ARF6-mediated endocytic recycling impacts cell movement, cell division and lipid homeostasis. *Semin Cell Dev Biol* 22:39–47.
- Jaworski J (2007) ARF6 in the nervous system. *Eur J Cell Biol* 86:513–524.
- Choi S, et al. (2006) ARF6 and EFA6A regulate the development and maintenance of dendritic spines. *J Neurosci* 26:4811–4819.
- Sakagami H, Matsuya S, Nishimura H, Suzuki R, Kondo H (2004) Somatodendritic localization of the mRNA for EFA6A, a guanine nucleotide exchange protein for ARF6, in rat hippocampus and its involvement in dendritic formation. *Eur J Neurosci* 19:863–870.